Structure determination for PF_3 absorption on Ni(111)

1992 J. Phys.: Condens. Matter 4 6509

(http://iopscience.iop.org/0953-8984/4/31/004)

J. Phys.: Condens. Matter 4 (1992) 6509–6522. Printed in the UK

Structure determination for PF_3 adsorption on Ni(111)

M Kerkar†, D P Woodruff†, J Avila‡, M C Asensio‡, M Fernández-Garcia§ and J C Conesa§

† Physics Department, University of Warwick, Coventry CV4 7AL, UK
‡ Instituto de Ciencia de Materiales, CSIC, Serrano 144, 28006 Madrid, Spain
§ Instituto de Catalisis y Petroleoquimica, CSIC, Campus Universidad Autonoma, Cantoblanco, 28049 Madrid, Spain

Received 29 May 1992

Abstract. The local adsorption structure of PF_3 on Ni(111) has been investigated using a combination of P K-edge near-edge and surface extended x-ray absorption fine structure (NEXAFS and SEXAFS) and normal incidence standing x-ray wavefield absorption (NISXW) at both the P and F atoms in order to determine the adsorption site, the adsorbate–substrate bond-length, the molecular orientation, and the internal structure of the adsorbed species. The molecule is found to be adsorbed atop a top layer Ni atom at a P–Ni nearest-neighbour distance of 2.07±0.03 Å, with its C_{3v} symmetry axis perpendicular to the surface, and with an internal structure (both bond-lengths and bond angles) unchanged from that of the free molecule. The results also indicate that there is no change in the Ni(111) substrate structure induced by the adsorption, and the PF_3 has a much larger vibrational amplitude parallel to the surface than perpendicular to the surface, presumably associated with a Ni–PF_3 wagging mode.

1. Introduction

Small molecules form a particularly important class of adsorbate species in studies of well-characterised surfaces because they are most directly relevant to improving our understanding of heterogeneous catalysis. They also provide a bridge to the chemistry of metal coordination compounds which are often considered to be valuable models for understanding metal surface chemistry [1]. In this context, phosphorus trifluoride, PF_3, is of particular interest [1] because its method of bonding to metal surfaces is believed to be very similar to that of CO (σ donation to the metal from the highest occupied molecular orbital, and π back-bonding from the metal into the highest unoccupied orbital of the molecule); CO, of course, is involved in many important catalytic processes and so its surface chemistry has been extensively investigated. One important difference between CO and PF_3, however, is that although adsorption strengths are very similar, PF_3 appears to form only linear bonds in coordination compounds, whereas CO is known to form linear, bridging (and higher coordination) bonds.

Although there is a growing literature concerning the adsorption of PF_3 on well-characterized metal surfaces [1–10], there appear to be no quantitative structural studies, and in particular no determination of the adsorption site which has been

0953-8984/92/316509+14$04.50

generally assumed to be atop in order to retain the linear geometry of the co-ordination compounds. There have, however, been several studies using electron stimulated desorption ion angular distributions (ESDIAD) which show that the PF_3 may be azimuthally ordered or azimuthally randomly located (or rotating) under different conditions, and these measurements also indicate that the molecule adsorbs with its three-fold rotation axis along the surface normal. In the case of azimuthally oriented phases, symmetry arguments indicate that the observed ESDIAD pattern is only consistent with atop adsorption [3], and theoretical calculations support this view [11, 12]. One further interesting feature of these ESD measurements is that they indicate that the molecule is very easily fragmented by electron (or appropriate photon [10]) beams, producing PF_2, PF and P fragments. In the present work, however, we have not pursued this very interesting aspect of the surface photochemistry, but rather have taken precautions to minimize damage and to study only the adsorption structure associated with the intact molecule.

We report here on measurements of the adsorption phase formed by PF_3 adsorbed on Ni(111) at saturation coverage (in an ordered (2×2) phase) using near-edge and surface extended x-ray absorption fine structure (NEXAFS and SEXAFS) and normal incidence standing x-ray wavefield absorption (NISXW) which allows us to obtain a rather complete structure determination. In particular, P K-edge NEXAFS allows us to establish the orientation of the adsorbed molecule, P K-edge SEXAFS allows us to determine the P–F and P–Ni nearest-neighbour distances and the adsorption site (and a further check on the molecular orientation). NISXW (including triangulation of two different standing wavefields) provides us with an entirely independent determination of the adsorption site and, in combination with the SEXAFS results, a measurement of the magnitude of the change in the layer spacing of the outermost substrate layers. In addition, the P–F layer spacing difference may be obtained from the NISXW so that, in combination with the SEXAFS value for the P–F bond-length, the internal molecular bond angles may be determined.

2. Experimental procedure

The experiments were performed at the Science and Engineering Research Council's (SERC's) Daresbury Laboratory using the SEXAFS experimental chamber and beamline on the Synchrotron Radiation Source (SRS). This beamline [13, 14] is equipped with a grazing incidence pre-focussing mirror, a two-crystal monochromator, and a conventional surface science spectrometer sample chamber, all sharing a common ultra-high vacuum environment. The main sample chamber is provided with the usual sample manipulation, heating and cooling facilities, and with a double-pass cylindrical mirror analyser (CMA) for conventional electron beam excited Auger electron spectroscopy as well as electron spectroscopy excited by the monochromated synchrotron radiation, and with low-energy electron diffraction (LEED) optics. The CMA axis is 90° from the incident x-ray beam axis in the same (horizontal) plane as the dominant polarization plane of the synchrotron radiation. A parameter of the synchrotron radiation beamline which is of some importance in the application of the SEXAFS and NEXAFS techniques, and which has not been included in the original instrumental papers [13, 14] is the degree of linear polarization. This is determined by the SRS itself, by the vertical acceptance aperture of the beamline optics, and by the polariztion modification effected by the reflections from the pre-focussing mirror

and the monochromating crystals. In the 2–4 keV photon energy range typically used in most experiments on this beamline the intrinsic degree of polarization accepting approximately ±0.13 mrad of vertical aperture is 87%, a figure only slightly modified by the 0.5° grazing reflection from the pre-mirror. The double reflection from the monochromator Ge(111) crystals, however, modifies this value in a significantly energy-dependent fashion because when the Bragg angle on these crystals is 45°, which occurs at a photon energy of 2796 eV, the out-of-plane polarization component is completely removed and the degree of polarization at the sample is 100%. This energy is close to the Cl K-edge, so SEXAFS and NEXAFS measurements at these energies are provided with a particularly ideal source [15, 16]. Similar calculations lead us to conclude that at the P K-edge the degree of linear polarization at the sample is 90%.

The Ni(111) sample was prepared by the usual combination of Laue x-ray alignment, spark machining, mechanical polishing and *in situ* argon ion bombardment and annealing until a clean well-ordered surface was obtained as judged by Auger electron spectroscopy and LEED. The PF_3 covered surface was prepared by exposing the clean surface at a temperature of 150 K to 5 L of PF_3 gas and briefly annealing the surface by heating to 250 K before allowing the surface to cool again for the x-ray measurements. This procedure, which is believed to achieve saturation coverage, is consistent with the preparation method reported by Alvey *et al* [3] to produce an ordered (2×2) phase with an assumed coverage of 0.25 ML [1–4]. In view of the reported (and our observed) sensitivity of this surface to electron beam damage, no Auger electron spectroscopy of LEED was performed prior to the x-ray measurements, but post-measurement observations confirmed that a (2×2) phase was produced.

SEXAFS and NEXAFS measurements were performed above the P K-edge around 2150 eV by monitoring with the CMA, the energy-filtered electron signal at 1855 eV corresponding to the P $KL_{2,3}L_{2,3}$ Auger electron peak. Spectra were recorded for grazing incidence angles of 20° and 90° (normal incidence). The NISXW measurements were conducted at normal incidence to the surface (111) planes and at normal incidence to the $(\bar{1}11)$ planes which lie at an angle of 70.5° to the surface in the appropriate (211) azimuth. The nominal energy of the normal incidence (111) Bragg reflection from Ni is 3045 eV and measurements were taken of the absorption in the P and F atoms of the adsorbate in these standing waves by monitoring the amplitude of the P and F 1s emissions at kinetic energies of approximately 895 eV and 2360 eV. Note that at the higher photon energy of the (111) Bragg peak the P $KL_{2,3}L_{2,3}$ Auger electron peak falls on the high-intensity inelastically scattered background of the Ni 2s and 2p photoemission peaks, leading to poor signal-to-background. The F 1s photoemission peak lies above these features, whilst the P 1s photoemission signal occurs at a kinetic energy well below those of the Ni 2s and 2p photoemission signals and just above the Ni KLL Auger peaks; both 1s photoemission peaks therefore offer quite good signal-to-background ratios and lie on rather flat parts of the electron energy spectrum. As in our previous applications of the NISXW technique [19, 20], the experiments involved four sequential photon energy scans through each Bragg reflection, measuring different emission signals, for each complete measurement of each species. These were the P (or F) 1s photoemission signal, the signal at a kinetic energy 50 eV higher which was used for background subtraction, the Ni L_3VV 845 eV Auger electron peak, and a similar kinetic energy background signal. The Ni signal is used to establish a reference of the substrate absorption of the standing wavefield which is used in fitting non-structural parameters as described in the next section.

3. Results and data analysis

3.1. SEXAFS

P K-edge SEXAFS spectra, recorded at normal and grazing incidence, are shown in figure 1 in the form of extracted fine structure functions (multiplied by k^2) versus k, the photoelectron wavevector. Also shown in this figure as broken curves are fits to these spectra obtained by a simulation using the EXCURV computer program [17, 18]. In the case of the normal emission spectrum, the fit is achieved using only one backscattering shell of F atoms at a distance of 1.54 Å. For grazing incidence, however, two shells are used which contribute very similar amplitude components; F at 1.53 Å and Ni at 2.07 Å. The fact that these two simulations provide a good description of the data (except for some deviation at the lowest energies) provides us with the core structural result. In particular, the observation that the Ni shell apparently contributes no discernible amplitude to the EXAFS at normal incidence implies that the nearest-neighbour Ni atom lies in a direction which is perpendicular to the polarization vector of the x-rays. As the latter lies in the surface plane (for all polarizations) at normal incidence, this tells us that the P–Ni nearest-neighbour direction is perpendicular to the surface and therefore the P atoms lie atop top layer Ni atoms, at a spacing of 2.07±0.03 Å, the limits of precision being typical of SEXAFS measurements of this kind [21, 22]. Since the P–F bond-length in the gas phase molecule is given in standard reference texts [23] as 1.535 Å, we also deduce that the distance is unchanged in the adsorbed species to within similar error limits set by our technique.

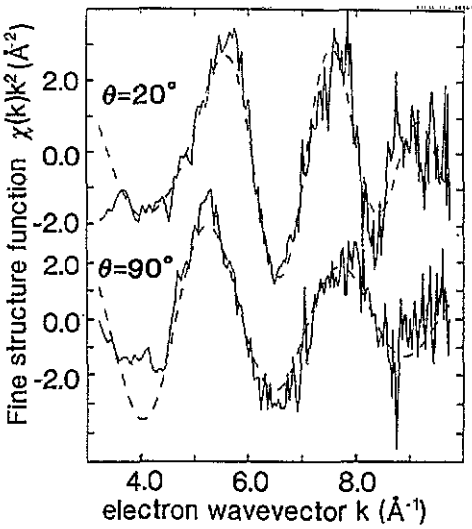

Figure 1. Experimental P K-edge SEXAFS from PF_3 adsorbed on Ni(111), measured at 20° grazing and normal incidence, shown in the form of the fine structure function multiplied by k^2 versus k, the photoelectron wavevector. The broken lines are one or two scattering shell fits as described in the text.

One further piece of information which is available from these fits is the angle of the P–F bond relative to the surface normal, which can be obtained from the polarization direction dependence of the F backscattering amplitude. Figure 2 shows

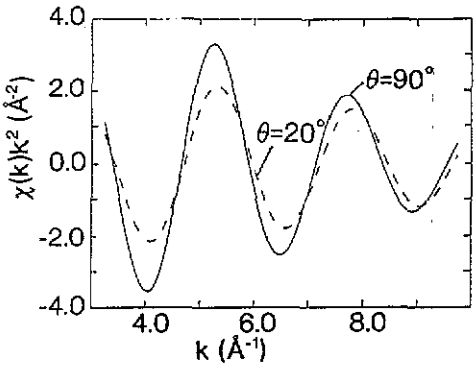

Figure 2. F backscattering contributions to the SEXAFS fits shown in figure 1.

the F shell backscattering contributions used in the fits shown in figure 1, and it is clear that the F atoms contribute slightly more to the EXAFS at normal incidence than at grazing incidence, indicating that the P–F bonds make an angle of more than the 'magic' angle (54.7°) relative to the surface normal [21, 22]. An average of several fits to different experimental spectra leads us to determine an amplitude ratio of normal to grazing incidence of 1.6±0.2. Applying the standard formula for the polarization angle dependence of the backscattering amplitude [21, 22] leads to a conclusion that the P–F bond angle relative to the surface normal is 62±2°. The surprising degree of accuracy applied by this result stems from the fact that the amplitude ratio is very strongly dependent on the bond angle when this angle falls close to the 'magic' angle at which the ratio is unity. Much lower accuracy is obtained when the bond angle is close to zero, a more commonly encountered situation. Note that for the same reason this deduction is insensitive to small amounts of vertical polarization in the incoming synchrotron radiation; in particular, the conclusion is indistinguishable, within the quoted error limits, for perfect and 90% polarization. As we note below, the NEXAFS results are far more sensitive to this parameter. We should finally note that the angle of 62° is in exact agreement with the angle that the P–F bond makes with the three-fold rotation axis of the free molecule (for which the F–P–F angle is 100° [23]), implying that the molecule is undistorted by adsorption, and is adsorbed with its symmetry axis perpendicular to the surface. This latter conclusion is obtained independently from the NEXAFS analysis described below.

3.2. NEXAFS

Figure 3 shows the P K-edge NEXAFS of this system recorded at normal and grazing incidence. The spectra are clearly dominated by three main features at approximately 2149 eV, 2153 eV and 2166 eV; note that the dependence on the angle of incidence of the two lowest energy states is very strong, but both features are clearly visible (simultaneously) in spectra recorded at intermediate incidence angles. In view of the analogous bonding behaviour of PF_3 and CO it seems likely that the intense feature at threshold (2149.5 eV) is associated with a transition to the lowest unoccupied 'π'-symmetry (strictly e-symmetry) orbital of the molecule, whilst one or both of the higher energy features is some kind of 'σ'-symmetry (a_1) scattering or quasi-bound ('shape') resonance. The P 1s excitation spectrum of the free molecule does not appear to have been measured previously, but Sodhi and Brion [24] have measured the

2s and 2p excitation spectra. In the case of the 2s (which has the same orbital angular momentum quantum number) they observe a single strong peak as the lowest energy feature (192.60 eV) which they also label as a transition to the lowest e-symmetry unoccupied state, but they also observe weaker structures some 3.6 eV higher in energy, and beyond, which they attribute to transitions to the lowest a_1 state and to Rydberg states; their 2s spectrum is not extended to sufficiently high energies to observe the highest energy (2166 eV) peak seen in our spectra, although a feature at a similar energy does appear in their 2p spectrum and could, perhaps, have the same origin. The similarity of the energy difference between the two lowest energy features in our 1s and Sodhi and Brion's 2s spectra indicates that they involve transitions to the same unoccupied states. Our assignment can be both tested and exploited to try to obtain molecular orientation information by quantifying the polarization angle dependence of the amplitude of these peaks, and particularly of the lowest (2149.5 eV) feature which we assign to an e-symmetry final state. Even without a quantitative analysis, figure 3 shows that the qualitative behaviour is consistent with the e and a_1 symmetry assignments to the two lower energy peaks, and with the orientation of the adsorbed species implied by the SEXAFS results. In particular, if the symmetry axis of the adsorbed molecule does lie perpendicular to the surface, transitions to an e-symmetry state should have their largest intensity at normal incidence, and zero intensity at true (0°) grazing incidence, whilst transitions to an a_1 state should have the opposite angular dependence. This behaviour is clearly consistent with the spectra of figure 3 if the two lowest energy features involve e and a_1 symmetry states, respectively, and indeed this argument indicates that the higher energy feature does not have any such simple single symmetry assigment.

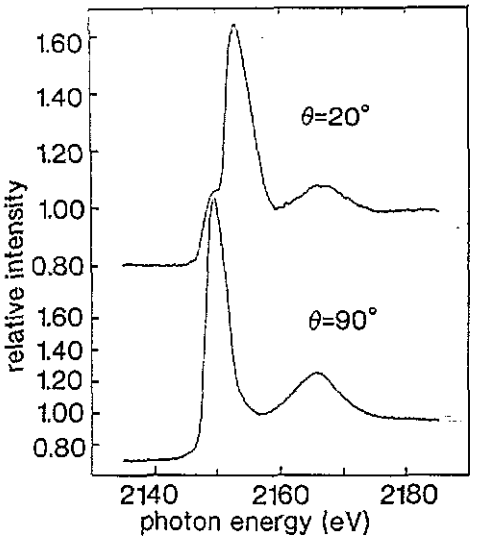

Figure 3. P K-edge NEXAFS spectra from PF_3 adsorbed on Ni(111), measured at 20° grazing and at normal incidence.

In order to quantify this further, however, it is necessary to extract the intensity of the observed peaks, and particularly of the sharp e-symmetry feature, as a function of the incidence direction from the data of figure 3, and this in turn necessitates

establishing the form of the background which lies under this peak. A key problem in this exercise, which has been discussed previously by Outka and Stöhr [25], is defining the location of the underlying edge jump in the spectrum; in particular, does the lowest energy (2149.5 eV) feature lie below or above this edge? Figure 4 illustrates the problem by showing the two possible edge locations and the two different excitation spectra which are obtained by using these different backgrounds. Clearly, the residual amplitude of the 2194.5 eV feature in the grazing incidence spectrum is very sensitive to this background choice. One piece of information which can clarify the proper choice is an accurate knowledge of the P 1s binding energy in the appropriate adsorption state [25], but in the present case a very careful calibration of the electron spectrometer was not undertaken so this information is not available with the necessary precision. Fortunately, when we try to use the amplitude information derived from the different background subtractions to obtain information on the molecular orientation we find that only one interpretation, that the first peak lies below the edge, is capable of consistent interpretation.

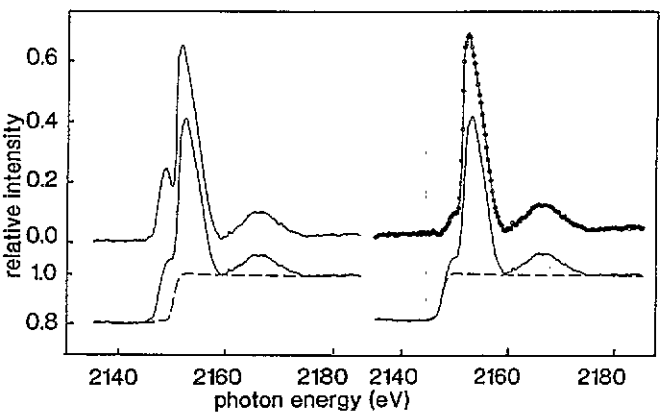

Figure 4. Possible background subtractions for the grazing incidence NEXAFS spectrum of figure 3. The lower curves show the (same) raw NEXAFS spectrum, and possible backgrounds, whilst the upper curves show the effect of subtracting these backgrounds.

In particular, we have already noted that the degree of linear polarization of the synchrotron radiation available on our beamline at the P K-edge is almost exactly 90%. This means that even if the molecular symmetry axis lies exactly perpendicular to the surface and one were to conduct an experiment at perfect (0°) grazing incidence, such that the dominant polarization lies perpendicular to the surface and thus is incapable of exciting transitions to an e-symmetry final state, the small component of the perpendicular polarization, which still lies in the surface plane, can lead to some intensity in such a feature. The actual intensity to be expected can readily be calculated as a function of the polarization direction because one simply samples the residual fraction of the component in the allowed geometry [21, 22]. Using these argument we find that at 90% polarization and 20° grazing incidence, transitions to an e-symmetry state should have an intensity of 15% of that at normal incidence. This is in good agreement with the experimental value obtained assuming that the first peak does involve an e-symmetry final state below the continuum edge jump and that the molecular symmetry axis lies along the surface normal. By contrast, if we assume the peak lies above the edge, the experimental intensity ratio is only 5%

which is too small to be reconciled even with these most extreme assumptions about the symmetry character.

In the present case, therefore, we are able to confirm our symmetry assignment of the lower spectra features, to establish that the molecule is adsorbed with no detectable tilt of its symmetry axis relative to the surface normal (the angular precision of this statement being typically $\pm 10°$ [21,22,25]), and coincidentally can also determine the edge-jump energy relative to the e-symmetry transition feature. Of course, these self-consistency arguments would not be applicable to a situation involving a lower symmetry adsorbate situation.

3.3. NISXW

The NISXW method, and the differences between this technique and the more conventional and older SXW method, have been discussed by some of us elsewhere in more detail [19,20,26–30]. We note here only that we measure the x-ray absorption in specific adsorbate atoms as a function of the exact photon energy as we scan through a Bragg scattering condition and the associated standing x-ray wavefield is shifted in a well-defined fashion relative to the substrate scatterer positions. By matching the observed absorption profiles to simple model calculations we obtain the spacing of the adsorbate atoms relative to the extended substrate scatterer planes in which the standing x-ray wavefield is established. If different (non-parallel) scattering planes are used, then the different layer spacings obtained can be used to determine the absolute site of the adsorbate atoms by simple real-space triangulation [27–30]. In the present case the main experimental results are summarised in figures 5 and 6 which show the Ni absorption profiles through the (111) and the ($\bar{1}11$) NISXW scattering conditions, together with the P (figure 5) and F (figure 6) absorption profiles.

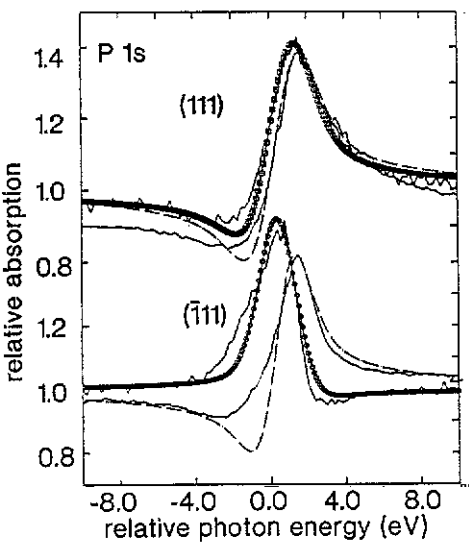

Figure 5. Ni and P absorption profiles recorded through the (111) and ($\bar{1}11$) NISXW conditions. The smooth lines are theoretical fits as described in the text.

The analysis of these data proceeds as in the earlier work cited above. Specifically, we fit theoretical calculations to the (Ni) substrate absorption profiles allowing the

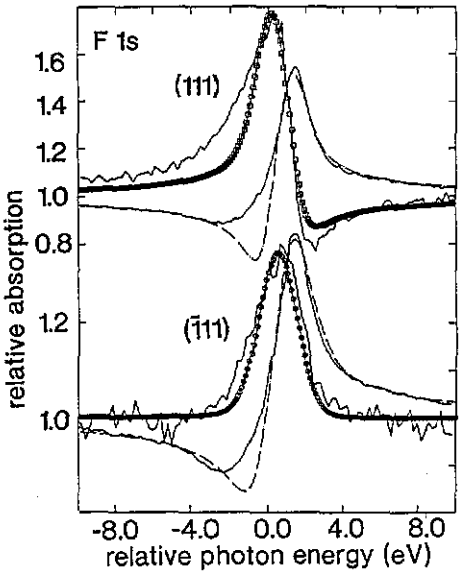

Figure 6. Ni and F absorption profiles recorded through the (111) and (1̄11) NISXW conditions. The smooth lines are theoretical fits as described in the text.

non-structural variables of the absolute energy and instrumental energy broadening to be adjusted, but assuming that all substrate absorbers are located at ideal substrate lattice sites except that the coherent fraction of such absorbers is varied if necessary. This parameter takes account of any static or enhanced dynamic disorder (we include the dynamic disorder associated with a bulk Debye–Waller factor, which introduces an incoherent element into the x-ray wavefield itself, separately). The adsorbate absorption profiles are then fitted using the same non-structural parameter values, the only variables now being the adsorbate layer spacing relative to the underlying substrate scatterer planes, and the adsorbate coherent fraction. The results of these fitting procedures are also included in figures 5 and 6 superimposed on the experimental data.

In the case of the P absorption measurements (figure 5) the fits to the substrate absorption were achieved using coherent fractions of 1.0 (111) and 0.9 (1̄11) whilst the P signals were fitted at (111) by a layer spacing of 0.1 Å and a coherent fraction of 0.8 and at (1̄11) by a layer spacing of 0.7 Å and a coherent fraction of 0.5. The small difference in the Ni coherent fractions is of marginal significance (we estimate an error of approximately ±0.1 in the coherent fractions) but we should note that the (1̄11) reflection is excited at relatively grazing incidence so that area of sample illuminated in the (111) and (1̄11) measurements is quite different. The very much lower coherent fraction for the (1̄11) reflection in the P adsorption profile, on the other hand, is clearly significant and is discussed further below. We should also remark on the slightly disappointing quality of some of the theoretical fits on the low-energy side of the absorption profiles seen in figures 5 and 6, particularly in the low-energy negative excursion seen from the substrate. The discrepancy seen here is actually rather characteristic of many of our previous measurements although in the present case the discrepancy is a little worse than before. The origin of this problem is unclear, but may be associated with the form of the included instrument function (notably the energy broadening) which we assume to have a symmetric Gaussian

lineshape; some assymmetry in this lineshape may lead to the observed difficulties, but there appears to be no simple way of measuring this directly. Nevertheless, the overall amplitude and energy location of the main absorption variations seen in these profiles indicates that the layer spacings obtained should still be accurate to no worse than ±0.1 Å.

In order to determine the adsorption site of the P atoms in the PF_3 from the (111) and ($\bar{1}11$) layer spacings we calculate the predicted ($\bar{1}11$) layer spacing which would be obtained using the measured (111) layer spacing and assuming occupation of one of the three possible high symmetry sites available on this surface. These are the two different three-fold coordinated hollow sites which lie directly above a Ni atom in the second layer ('HCP') or the third layer ('FCC'), and atop. We should first note, however, that because the standing x-ray wavefield is established in the underlying bulk (the x-rays penetrate far into the solid relative to the top few layers of interest to us in surface science), the layer spacings obtained are ambiguous in that we may add any integral number of substrate layer spacings (2.03 Å) to them. Reasonable assumptions concerning the nearest-neighbour distances, however, typically allow us to remove this ambiguity. In the present case we note that the measured 0.10±0.10 Å (111) layer spacing is extremely small, and that a value one substrate layer spacing larger (2.33±0.10 Å) is much more likely. If we take this larger value, the predicted ($\bar{1}11$) spacings compatible with this are 0.71±0.03 Å (atop), 0.03±0.03 Å (FCC) and 1.40±0.03 Å (HCP). Clearly the only one of these which is consistent with the experimentally measured ($\bar{1}11$) layer spacing of 0.70±0.10 Å is atop. Note that if we do use the smaller (111) layer spacing of 0.10 Å, identical arguments lead to the conclusion that the adsorption site is HCP, a site which is directly atop (by 2.13 Å) a *second* layer Ni atom. This discussion highlights the fact that the NISXW triangulation determines the adsorbate site relative to the underlying substrate uniquely, but the *local* site depends on assumptions concerning the location of the outermost substrate layers relative to this adsorbate location. In particular, the NISXW data is unaffected by adding or subtracting substrate layers between (or beyond) the adsorbate and underlying substrate layers.

In the present case, we can exclude the 0.0 Å layer spacing HCP site (on an ideally terminated substrate) because this would imply a P–Ni nearest-neighbour distance of 1.44 Å and thus an effective radius for the adsorbed P of 0.20 Å, quite unreasonably small. Similarly larger layer spacings (e.g. 4.16 Å in an FCC site) lead to unacceptably large P–Ni nearest-neighbour distances. The NISXW result therefore leads to the conclusion that the P atoms are located atop top layer Ni atoms at a layer spacing of 2.13±0.10 Å, which is in excellent agreement with the SEXAFS result.

A further important piece of information emerging from the P NISXW which we have not yet discussed is the value of the coherent fraction parameter obtained from the (111) and ($\bar{1}11$) Bragg reflection conditions. As we have already remarked, this parameter is a measure of the combined effects of the static and dynamic disorder of the P locations (being unity for perfect disorder and zero for random positions) and, as the order is measured perpendicular to the relevant scattering plane, the (111) NISXW provides information on the order perpendicular to the surface whereas the ($\bar{1}11$) samples positional variation along a direction at 70.5° to the surface normal and is therefore predominantly influenced by disorder parallel to the surface. Note that the order is measured relative to the underlying bulk scatterer planes, and is therefore not influenced by near-neighbour correlated vibrations as is a local scattering technique such as SEXAFS or photoelectron diffraction [31]. The coherent fraction

values for the P absorbers of 0.8 for (111) and 0.5 for ($\bar{1}11$) therefore imply a very much enhanced disorder parallel to the surface; whilst we cannot, using these fixed temperature experimental data, formally exclude the possibility that this difference is associated with static disorder, the tendancy of the system to form a well-ordered (2×2) superstructure suggests that the static order parallel to the surface is good, and that the origin is therefore dynamic. In particular, the atop adsorption site may be expected to lead to a soft Ni–PF_3 wagging vibration, and the large amplitude of this vibration can then account for the low ($\bar{1}11$) coherent fraction. Indeed, if we convert this coherent fraction value to a dynamic (Debye–Waller-like) effect, we conclude that the root mean square vibrational amplitude of the P atoms parallel to the surface is 0.27±0.04 Å. This interpretation of a large wagging vibrational mode for an atop adsorbed species is consistent with our earlier NISXW findings for Rb on Al(111) [27,28], and with photoelectron diffraction measurements for NH_3 on Ni(111) [32].

In the case of the F NISXW absorption profiles shown in figure 6, the associated theoretical fits also shown in this figure have associated structural parameter values of: Ni coherent fractions, 1.0 for (111) and 0.8 for ($\bar{1}11$); F–Ni layer spacings, 0.85 Å for (111) and 0.6 Å for ($\bar{1}11$); F coherent fractions, 0.95 for (111) and 0.1 for ($\bar{1}11$). Clearly the (111) measurements both have good associated coherent fractions, so the F–Ni layer spacing is well-defined, a result which would be difficult to reconcile with PF_3 adsorbed in anything but the most symmetric arrangement with its symmetry axis along the surface normal. We also note that the F–Ni layer spacing obtained perpendicular to the surface is 0.75±0.15 Å larger than the P–Ni spacing (taking the precision in both adsorbate–Ni layer spacings as ±0.10 Å). This is to be compared with the fact that, in the free PF_3 molecule, the P–F distance, projected onto the three-fold rotation axis of the molecule, is 0.72 Å. Clearly these results therefore further reinforce the SEXAFS and NEXAFS conclusions that the molecule is adsorbed in this symmetry orientation with no detectable distortion of its internal structure.

The principal result derived from the F ($\bar{1}11$) NISXW is that the coherent fraction is not significantly different from zero. Notice in this context that the 0.6 Å absorption profile has almost the same lineshape as the entirely incoherent (reflectivity) profile, although the modulation amplitude is different. Bearing in mind our estimated precision for the coherent fractions of ±0.1, any difference between our best fit and that of total incoherence is marginal. This result is most easily reconciled with the idea that the adsorbed PF_3 molecules are not azimuthally ordered, but either randomly located or freely rotating about the molecular symmetry axis; in this situation the anticipated coherent fraction for the ($\bar{1}11$) NISXW would, indeed, be indistinguishable from zero. We note too that the ESDIAD measurements on this adsorption system [2,3] do show this lack of azimuthal order at room temperature. On the other hand, these same ESDIAD studies show that at 85 K good azimuthal order is obtained at high coverage, with the projection of the PF bonds onto the surface aligned along the (110) direction. Using our known internal structure of the PF_3 molecule, this adsorbate–substrate conformation actually places the F atoms almost in (0.10 Å off) bridge sites relative to the underlying Ni atoms. Even in this well-ordered state, however, SXW would be expected to show a much reduced coherent fraction for the ($\bar{1}11$) reflection; this is because even the symmetric bridge site has reduced symmetry relative to the substrate (the 3-fold rotation axis is lost and only the mirror plane remains), so the ($\bar{1}11$) SXW averages over three inequivalent sites. Coupled with the fact that the F atoms are slightly off the true bridge sites, this domain averaging will reduce the coherent fraction further; estimates suggest that the final result *should* be

distinguishable from a totally incoherent signal, but as the average layer spacing of the coherent component is calculated to be approximately 0.65 Å for this situation (a layer spacing which we have already remarked gives a rather similar SXW lineshape to that of zero coherence), it is clear that our ability to distinguish the azimuthally ordered and disordered phases is marginal. We therefore conclude that the extremely low coherent fraction seen for the F ($\bar{1}11$) absorption profile is consistent with our expectations for either azimuthally ordered or disordered phases, although the latter conclusion is marginally favoured.

4. Discussion and conclusions

Clearly the combined results of the SEXAFS, NEXAFS and NISXW provide a rather complete picture of the adsorption geometry of PF_3 on Ni(111) in which most aspects of the structure are confirmed independently by at least two methods. In particular all three methods provide evidence that the PF_3 adsorbs with its symmetry axis aligned along the surface normal, SEXAFS giving the expected P–F bond angle relative to the surface, NEXAFS defining the symmetry axis orientation directly, and NISXW confirming the result via the P–F layer spacing perpendicular to the surface. The SEXAFS P–F bond angle and bond-length, and the NISXW P–F bond-length projected along the surface normal, also confirm that the PF_3 is undistorted by its interaction with the metal. Finally, both SEXAFS and NISXW confirm the atop site adsorption geometry.

The essential equivalence of the SEXAFS Ni–P nearest-neighbour distance (2.07±0.03 Å) and the NISXW P–Ni layer spacing (2.13±0.10 Å) have a slightly greater significance than one might first suppose because the two techniques measure different physical parameters. Specifically, SEXAFS measures the true *local* adsorbate–substrate distance, whereas NISXW measures the adsorbate location relative to the extension of the substrate scatterer planes and thus determines the local spacing only for an ideally-terminated solid. This means that if there is any net (integrated) change in the substrate (Ni–Ni) layer spacings in the outermost layers, the SEXAFS and NISXW layer spacings should differ by this amount. Formally, therefore, the combination of the two measurements actually leads to the conclusion that the outermost layers of the substrate are expanded by 0.06±0.10 Å, or in effect that there is no change within the limits of precision of our measurements. In truth this is not entirely surprising as the FCC (111) (close-packed) metal surfaces typically show little or no detectable outermost layer relaxation in their clean state [33].

One further piece of information which we have extracted from our measurements concerns the degree of local order which is most probably associated with vibrational and rotational states. Our implication from the NISXW that the PF_3 is not azimuthally ordered, and is probably freely rotating, is generally consistent with prior ESDIAD work which has studied this aspect in some detail [2,3]. An entirely new result, however, concerns the enhanced vibrational amplitude parallel to the surface which appears to be characteristic of atop bonded wagging vibrations. New photoelectron diffraction measurements, conducted over a range of sample temperatures, provide *direct* confirmation of this effect [34].

In view of the early comments concerning the connection of coordination chemistry and surface science, it is also interesting to remark on the adsorption site and bond-length. This is the first quantitative site determination for PF_3 adsorbed on a metal surface, although atop adsorption has previously been inferred and theoretically

predicted, and in this first case at least, the molecule does adopt a singly coordinated site as found uniquely in coordination compounds. There have also been measurements of Ni–P bonding distances in Ni/PF_3 compounds which are in excellent accord with our findings for the Ni(111) surface; in particular in $Ni(PF_3)_4$ the Ni–P distance has been found to be in the range 2.10–2.11 Å, [35], very close to our measurement for $Ni(111)/PF_3$ of 2.07±0.03 Å.

Acknowledgments

The authors are pleased to acknowledge the support of the SERC and of the European Commission, under both the SCIENCE and Large Scale Installations programmes for financial assistance including access to the SRS at Daresbury Laboratory.

References

[1] Nitschké F, Ertl G and Küppers J 1981 *J. Chem. Phys.* **74** 5911
[2] Alvey M D, Yates J T Jr and Uram K J 1987 *J. Chem. Phys.* **87** 7221
[3] Alvey M D and Yates J T Jr 1988 *J. Am. Chem. Soc.* **110** 1782
[4] Guo X, Yates J T Jr, Agrawal V K and Trenary M 1991 *J. Chem. Phys.* **94** 6256
[5] Liang S and Trenary M 1988 *J. Chem. Phys.* **89** 3323
[6] Shanahan K L and Muetterties E L 1984 *J. Chem. Phys.* **88** 1996
[7] Zhou Y, Mitchell G E, Henderson M A and White J M 1989 *Surf. Sci.* **214** 209
[8] Johnson A L, Joyce S A and Madey T E 1988 *Phys. Rev. Lett.* **61** 2578
[9] Joyce S A, Johnson A L and Madey T E 1989 *J. Vac. Sci. Technol.* A **7** 2221
[10] Joyce S A, Yarmoff J A and Madey T E 1991 *Surf. Sci.* **254** 144
[11] Doyen G 1982 *Surf. Sci.* **122** 505
[12] Chan A W E and Hoffman R 1990 *J. Chem. Phys.* **92** 699
[13] MacDowell A A, Norman D, West J B, Campuzano J C and Jones R G 1986 *Nucl. Instrum. Methods* A **246** 131
[14] MacDowell A A, Norman D and West J B 1986 *Rev. Sci. Instrum.* **57** 2667
[15] Kerkar M, Walter W K, Woodruff D P, Jones R G, Ashwin M J and Morgon C 1992 *Surf. Sci.* **268** 36
[16] Norman D 1991 private communication
[17] Gurman S J 1980 *Technical Memo No DL/SCI/TM21T* (SERC Daresbury Laboratory, Warrington, UK)
[18] Gurman S J, Binsted N and Ross I 1984 *J. Phys. C: Solid State Phys.* **17** 143
[19] Woodruff D P, Seymour D L, McConville C F, Riley C E, Crapper M D, Prince N P and Jones R G 1987 *Phys. Rev. Lett.* **54** 1460
[20] Woodruff D P, Seymour D L, McConville C F, Riley C E, Crapper M D, Prince N P and Jones R G 1988 *Surf. Sci.* **195** 237
[21] e.g., Stöhr J 1988 *X-ray Absorption Principles, Techniques and Applications of EXAFS, SEXAFS and XANES* ed R Prins and D C Kongsberger (New York: Wiley) 443
[22] Woodruff D P 1986 *Rep. Prog. Phys.* **49** 683
[23] *Handbook of Chemistry and Physics* (West Palm Beach, FL: Chemical Rubber)
[24] Sodhi R N S and Brion C E 1985 *J. Electron. Spectrosc. Relat. Phenom.* **37** 97
[25] Outka D and Stöhr J 1988 *J. Chem. Phys.* **88** 3539
[26] Prince N P, Ashwin M J, Woodruff D P, Singh N K, Walter W and Jones R G 1990 *Faraday Discuss. Chem. Soc.* **89** 301
[27] Kerkar M, Fisher D, Woodruff D P, Jones R G, Diehl R D and Cowie B 1992 *Phys. Rev. Lett.* **68** 3204
[28] Kerkar M, Fisher D, Woodruff D P, Jones R G, Diehl R D, McConville C F and Cowie B 1992 *J. Vac. Sci. Technol.* A **10** at press
[29] Kerkar M, Fisher D, Woodruff D P and Cowie B 1992 *Surf. Sci.* at press

[30] Kerkar M, Hayden A B, Woodruff D P, Kadodwala M and Jones R G 1992 *J. Phys.: Condens. Matter* **4** 5043
[31] e.g., Woodruff D P 1986 *Surf. Sci.* **166** 387
[32] Fritzsche V, Schindler K-M, Gardner P, Bradshaw A M, Asensio M C and Woodruff D P 1992 *Surf. Sci.* **269/270** 35
[33] MacLaren J M, Pendry J B, Rous P J, Saldin D K, Somorjai G A, Van Hove M A and Vvedensky D D 1987 *Surface Crystallographic Information Service: A Handbook of Surface Structures* (Dordrecht: Reidel)
[34] Dippel R, Weiss K-U, Hu X M, Schindler K-M, Gardner P, Asensio M C, Fritsche V, Woodruff D P and González-Elipe A R to be published
[35] Almenningen A, Andersen B A and Astrup E E 1970 *Acta. Chem. Scand.* **24** 1579